

## Metadata of the chapter that will be visualized online


Chapter Title	Remote Sensing-Based Assessment of Mangrove Ecosystem with Special Reference to the Sundarbans of India	
Copyright Year	2026	
Copyright Holder	The Author(s), under exclusive license to Springer Nature Switzerland AG	
Corresponding Author	Family Name	<b>Barman</b>
	Particle	
	Given Name	<b>Dhananjay</b>
	Suffix	
	Division	
	Organization/University	ICAR—Central Research Institute for Jute and Allied Fibres
	Address	Kolkata, India
Author	Family Name	<b>Srivastava</b>
	Particle	
	Given Name	<b>Sanjeev Kumar</b>
	Suffix	
	Division	
	Organization/University	University of the Sunshine Coast
	Address	Sippy Downs, QLD, Australia
Author	Family Name	<b>Kar</b>
	Particle	
	Given Name	<b>Gouranga</b>
	Suffix	
	Division	
	Organization/University	ICAR—Central Research Institute for Jute and Allied Fibres
	Address	Kolkata, India
Author	Family Name	<b>Banerjee</b>
	Particle	
	Given Name	<b>Saon</b>
	Suffix	
	Division	
	Organization/University	Bidhan Chandra Krishi Viswavidyalaya
	Address	Mohanpur, India

Author	Family Name	<b>Banik</b>
	Particle	
	Given Name	<b>Debangana</b>
	Suffix	
	Division	
	Organization/University	ICAR—Central Research Institute for Jute and Allied Fibres
	Address	Kolkata, India
Author	Family Name	<b>Basak</b>
	Particle	
	Given Name	<b>Bulu</b>
	Suffix	
	Division	
	Organization/University	ICAR—Central Research Institute for Jute and Allied Fibres
	Address	Kolkata, India
Author	Family Name	<b>Arfin-Khan</b>
	Particle	
	Given Name	<b>S. A.</b>
	Suffix	
	Division	
	Organization/University	Shahjalal University of Science and Technology
	Address	Sylhet, Bangladesh
Author	Family Name	<b>Mukul</b>
	Particle	
	Given Name	<b>Sharif A.</b>
	Suffix	
	Division	
	Organization/University	United International University
	Address	Dhaka, Bangladesh
Author	Family Name	<b>Arief</b>
	Particle	
	Given Name	<b>M. C. W.</b>
	Suffix	

	Division	
	Organization/University	Universitas Padjadjaran
	Address	Jawa Barat, Indonesia
Author	Family Name	<b>Hindersah</b>
	Particle	
	Given Name	<b>Reginawanti</b>
	Suffix	
	Division	
	Organization/University	Universitas Padjadjaran
	Address	Jawa Barat, Indonesia
Abstract	<p>Mangrove forests are unique ecosystems that exist on tropical and subtropical coastal wetlands throughout the world. They provide multiple ecosystem services which are ecologically and economically beneficial to the planet by providing food and fodder, fish and shrimp breeding, protection from cyclones, coastal erosion, and saltwater intrusion, providing medicinal ingredients, and attracting tourists. However, these mangrove ecosystems face multiple facets of climatic, ecological, and anthropogenic threats of extinction. The area under mangrove forest has drastically reduced over the time. For the protection and conservation of the mangrove forests, there is an urgent need for accurate mapping of mangrove area and assessment of their vulnerability to climate change, and other abiotic, biotic, and anthropogenic threats. The remote sensing technique can play a vital role in assessing and providing spatiotemporal information on mangrove ecosystem distribution, species differentiation, health status, and ongoing changes of mangrove cover. Due to difficulty in accessing the mangrove areas by humans, various studies have been conducted by using different remote sensing techniques ranging from aerial photography to high- and medium-resolution optical imagery and from hyperspectral data to active microwave (SAR) data. Numerous scientific papers have reported studies on mangrove mapping, distribution, and health status over the last few decades. This chapter will primarily present how remote sensing techniques have been utilized by various researchers to address the multiple factors related to mangrove studies, including the Sundarbans mangrove of India, which is a UNESCO World Heritage site.</p>	
Keywords (separated by “ - ”)	<p>Mangrove forest - Remote sensing of mangrove - Coastal ecosystem mapping - Reflectance and backscattering properties of mangroves - Disaster mapping for mangrove</p>	

# Remote Sensing-Based Assessment of Mangrove Ecosystem with Special Reference to the Sundarbans of India

1  
2  
3

Dhananjay Barman, Sanjeev Kumar Srivastava , Gouranga Kar,  
Saon Banerjee, Debangana Banik, Bulu Basak, S. A. Arfin-Khan,  
Sharif A. Mukul, M. C. W. Arief, and Reginawanti Hindersah

4  
5  
6

**Abstract** Mangrove forests are unique ecosystems that exist on tropical and sub-tropical coastal wetlands throughout the world. They provide multiple ecosystem services which are ecologically and economically beneficial to the planet by providing food and fodder, fish and shrimp breeding, protection from cyclones, coastal erosion, and saltwater intrusion, providing medicinal ingredients, and attracting tourists. However, these mangrove ecosystems face multiple facets of climatic, ecological, and anthropogenic threats of extinction. The area under mangrove forest has drastically reduced over the time. For the protection and conservation of the mangrove forests, there is an urgent need for accurate mapping of mangrove area and assessment of their vulnerability to climate change, and other abiotic, biotic, and anthropogenic threats. The remote sensing technique can play a vital role in assessing and providing spatiotemporal information on mangrove ecosystem distribution, species differentiation, health status, and ongoing changes of mangrove cover. Due to difficulty in accessing the mangrove areas by humans, various studies have been conducted by using different remote sensing techniques ranging from aerial photography to high- and medium-resolution optical imagery and from hyperspectral data to active microwave (SAR) data. Numerous scientific papers have reported studies on mangrove mapping, distribution, and health status over the last few decades. This

7  
8  
9  
10  
11  
12  
13  
14  
15  
16  
17  
18  
19  
20  
21  
22  
23  
24

---

D. Barman (✉) · G. Kar · D. Banik · B. Basak  
ICAR—Central Research Institute for Jute and Allied Fibres, Kolkata, India

S. K. Srivastava  
University of the Sunshine Coast, Sippy Downs, QLD, Australia

S. Banerjee  
Bidhan Chandra Krishi Viswavidyalaya, Mohanpur, India

S. A. Arfin-Khan  
Shahjalal University of Science and Technology, Sylhet, Bangladesh

S. A. Mukul  
United International University, Dhaka, Bangladesh

M. C. W. Arief · R. Hindersah  
Universitas Padjadjaran, Jawa Barat, Indonesia

© The Author(s), under exclusive license to Springer Nature  
Switzerland AG 2026

79

S. K. Srivastava et al. (eds.), *Earth Observation for Monitoring Mangrove Ecosystems*, [https://doi.org/10.1007/978-3-032-16668-5\\_5](https://doi.org/10.1007/978-3-032-16668-5_5)

chapter will primarily present how remote sensing techniques have been utilized by various researchers to address the multiple factors related to mangrove studies, including the Sundarbans mangrove of India, which is a UNESCO World Heritage site.

**Keywords** Mangrove forest · Remote sensing of mangrove · Coastal ecosystem mapping · Reflectance and backscattering properties of mangroves · Disaster mapping for mangrove

## 1 Introduction

Mangrove forests exist on tropical and subtropical coastal wetlands throughout the world (Chapman, 1976; Tomlinson, 2016). They are among the most biologically important ecosystems on the planet. Mangrove forests consist of trees, shrubs, and fern species (Duke et al., 1998) that have adapted to the harsh conditions of high salinity, anoxic soils, warm air and water temperatures, high tides, and muddy waters. These ecosystems act as a first line of defence against tropical and subtropical cyclones, hurricanes, and tsunamis by dissipating wave and wind energy. Moreover, the mangrove ecosystems provide tremendous ecological and economic services to mankind by providing food, fodder, fuel, medicine, recreation, etc. This also helps to regulate the environment by absorbing atmospheric carbon di-oxide, stabilizing coastlines, and protecting against storms. According to Barbier et al. (2011), the benefits from carbon sequestration depend on factors like the density of their biomass and the price of carbon in the market which can vary extensively ranging from around \$60 to more than \$1000 per hectare each year. Additionally, the storm protection it offers has been valued from \$300 to as high as \$9000 per hectare annually. In the Sundarbans, research showed that local communities gain substantial economic benefits from mangroves and are open to investing in their conservation. For instance, Iqbal (2020) used a choice experiment approach to estimate the marginal willingness to pay (MWTP) for improvements in ecosystem services. Also, Mukherjee et al. (2014) emphasized light on the ecological and economic trade-offs in the mangrove forests of South Asia, underscoring the importance of integrated valuation in policymaking and land-use planning. Even though there are obstacles like hypothetical bias, limited data, and challenges in capturing cultural services, these valuation efforts play a vital role in shaping Payment for Ecosystem Services (PES) initiatives, blue carbon strategies, and adaptive climate policies.

However, these mangrove ecosystems face multi-facets of climatological, ecological, and anthropogenic threats of extinction. Many parts of the ecosystems have immersed into sea water because of the sea-level rise due to global warming. The regeneration capacity of mangroves has been overtaken by the more frequent cyclonic events. Many parts of the mangrove forests have been degraded polluted

and have lost biodiversity. Biodiversity in mangrove forests is increasingly at risk. In estimation, 1533 species are associated with mangroves, 15% of which are threatened with extinction. UNEP's report 'Decades of Mangrove Forest Change: What does it mean for nature, people and the climate?' found that nearly 50% of mangrove-associated mammals, 22% of fishes, 16% of plants, 13% of amphibians, and 8% of bird and reptile species are threatened with extinction. Worryingly, for 44% of the species, their extinction risk is increasing and of those already at risk, the situation is getting worse for 89%.

For addressing these issues and challenges, a proper and systematic assessment of the mangrove ecosystems is essential. As the manual survey and assessment is very difficult, and in some places, it is almost impossible due to the rough and tough characteristics of the ecosystems, satellite and unmanned aerial vehicle (UAV) can play a vital role in assessing the mangrove ecosystem. Many researchers worldwide have applied these techniques to assess the health of the mangrove ecosystem. These techniques in combination with modern-day artificial intelligence (AI) and machine learning (ML) techniques can provide even more real-time data in framing better management strategies for the mangrove ecosystems.

## 2 Global Distribution and Current State of the Mangrove Ecosystem

The global area of mangrove forest has been estimated to 147,359 km<sup>2</sup> (Global Mangrove Watch, 2020), 51% of which occurred in the Asia-Pacific, with 29% in the Americas, and 20% in Africa. Over the 24-year period from 1996 to 2020, it has been reported that the global mangrove forest cover has lost in the extent of 5245 km<sup>2</sup> (3.4%). However, in a latest assessment of UNEP using current satellite imagery, the global loss of mangroves has stabilized, and the mangrove cover increased in and around world's large rivers, estuaries, and deltas (UNEP, 2023).

According to the Global Forest Resource Assessment 2020 (FRA, 2020), 113 nations throughout the world have mangrove forests covering an estimated 14.72 million hectares. Asia has the highest documented mangrove area (5.33 million hectares), followed by South America (2.12 million hectares), Western and Central Africa (2.30 million hectares), North and Central America (2.55 million hectares), and Oceania that is claimed to have the least area of mangroves (1.26 million hectares). As per FRA 2020 report (Table 1), the global mangrove-cover between 1990 and 2020 declined from 15,759 hectares (157,590 km<sup>2</sup>) to 14,717 hectares (147,170 km<sup>2</sup>). Asia experienced the most significant loss, particularly in South and Southeast Asia (12.9%), where factors such as urbanization, aquaculture, and coastal development contributed to a loss of nearly 800 thousand hectares. Africa experienced a mild decrease, particularly in its western and central areas (4.6%), while Eastern and Southern Africa started to show a bit of recovery by 2020. Oceania, on the other hand, faced a net loss of 13.7%, even though there was some

**Table 1** Global status of the mangrove cover

Region/subregion	Mangrove area (1000 ha)			
	1990	2000	2010	2020
Eastern and Southern Africa	929	902	883	905
Northern Africa	34	31	32	31
Western and Central Africa	2436	2400	2349	2304
Total Africa	3398	3332	3264	3240
East Asia	24	22	25	32
South and Southeast Asia	6117	6108	5713	5330
Western and Central Asia	190	190	190	184
Total Asia	6331	6320	5928	5545
Total Europe	0	0	0	0
Caribbean	787	789	774	891
Central America	492	482	483	466
North America	1152	1167	1190	1195
Total North and Central America	2431	2439	2447	2552
Total Oceania	1447	1150	1314	1255
Total South America	2152	2050	1976	2124
World	<b>15,759</b>	<b>15,292</b>	<b>14,928</b>	<b>14,717</b>

Source: FRA (2020), FAO

103 improvement noted in 2010. However, according to FSI Report 2023, India ranks as  
 104 the world's third richest nation in terms of mangrove plant diversity, trailing behind  
 105 Indonesia and Australia. More than 40% of the total area of mangroves was found  
 106 to be in only four countries: Indonesia (19%), Brazil (9%), Nigeria (7%), and  
 107 Mexico (6%). The status of world mangrove cover in 2024 shows that Southeast  
 108 Asia has the largest share of mangrove cover, making up 33.6% of the total cover,  
 109 followed by North and Central America and the Caribbean (14.4%), South America  
 110 (13.2%), and West and Central Africa (15.5%). East and Southern Africa (5.3%),  
 111 South Asia (6.6%), and Australia and New Zealand (7.0%) are other regions with  
 112 moderate coverage. On the other hand, mangrove cover is comparatively low in the  
 113 Pacific Islands (3.9%), the Middle East (0.2%), and East Asia (0.2%) (Fig. 1).

### 114 3 Climatic Variability of Mangrove Ecosystems

115 Climate change and its variability can significantly impact on mangrove ecosys-  
 116 tems, which depend on species sensitivity and location (Randhir et al., 2024; Ward  
 117 et al., 2016). Changes in temperature and rainfall due to climate change affect  
 118 growth and development stages of mangrove species, leading to variations in leaf  
 119 area index (LAI) resulting changes in remotely sensed indices (e.g. Normalized  
 120 Difference Vegetation Index, NDVI; Enhanced Vegetation Index, EVI) if data is not  
 121 captured during peak biomass (Ganguly et al., 2012). Climate-driven shifts in

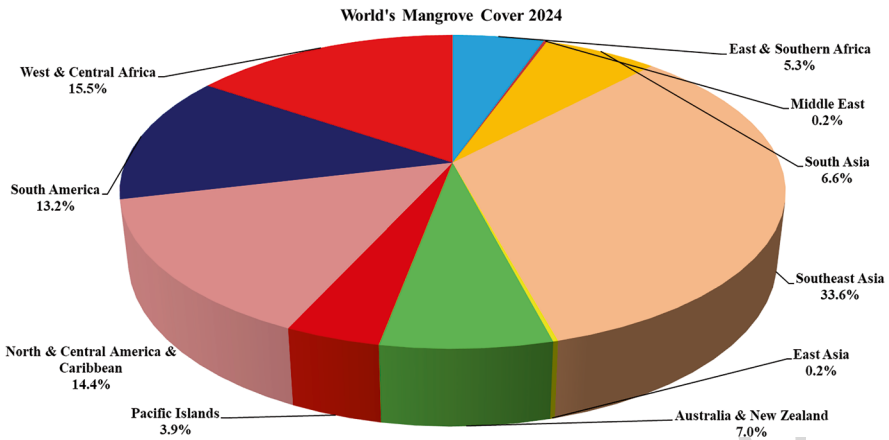


**Fig. 1** The current status of the world's mangrove cover. [Source: The State of the World's Mangroves 2024]

species composition and structure alter spectral reflectance, reducing the accuracy of biomass models based on historical data (Clark et al., 2003). In tropical regions like the Sundarbans, increased cloud cover and atmospheric disturbances degrade optical sensor data quality, thus making it difficult for monitoring and assessment of the mangrove ecosystem (Baccini et al., 2017). The effects of climate change on three dominant mangrove species globally: red, black, and white mangroves, were studied using simulation, GIS, and statistical modelling and revealed that low precipitation can impact growth of all three mangrove species, where even 1 mm reduction in precipitation decreased the growth suitability of red, black, and white mangroves by 0.008%, 0.004%, and 0.008%, respectively (Randhir et al., 2024). The Intergovernmental Panel on Climate Change (IPCC) in 2013 reported that the global sea levels are likely to rise by between 0.28 and 0.98 m by 2100 which will cause coastal flooding in future. In recent decades, global sea-level rise has been reported at the rate of  $3.2 \pm 0.4$  mm per year (Church & White, 2011). However, regional factors influence its variability from 1.9 mm per year in the Caribbean to 7.5 mm per year in parts of Indonesia (Nerem et al., 2010) and up to 9 mm per year in the lower Mississippi River Delta (NOAA, 2015). Sea-level rise can cause harm to mangrove by increasing inundation duration which leads to plant death (He et al., 2007) and shifting in species composition (Gilman et al., 2008). Sea-level rise and associated danger of sinking of mangrove area should be monitored periodically by using remote sensing (RS) data for taking appropriate climate action. Keeping in view the importance of the climate, an account of climatic situation of the major mangrove regions is presented in the Table 2.

122  
123  
124  
125  
126  
127  
128  
129  
130  
131  
132  
133  
134  
135  
136  
137  
138  
139  
140  
141  
142  
143  
144

**Table 2** Climate of the mangrove regions of different countries of the world

Country	Area (in ha)	% global total	Rainfall (mm)	Temperature range (°C)	RH (%)	Tidal influence (m)
Indonesia	3,112,989	22.6	2000–4000	25–30	≥80	Semi-diurnal (1–3)
Australia	977,975	7.1	1000–3500	24–30	≥70	Intertidal (2–4)
Brazil	962,683	7.0	1500–2500	25–30	≥80	Semi-diurnal (2–4 and ≥4)
Mexico	741,917	5.4	1000–2500	25–30	≥80	Semi-diurnal (1–2 and ≥3)
Nigeria	653,669	4.7	1500–3000	26–30	≥80	Semi-diurnal (1–2)
Malaysia	505,386	3.7	2000–4000	25–32	≥80	Semi-diurnal (1–3)
Burma (Myanmar)	494,584	3.6	1500–5000	25–32	≥80	Semi-diurnal (2–4)
Papua new Guinea	48,121	3.5	2000–3500	26–30	≥80	Semi-diurnal (1.5–4)
Bangladesh	436,570	3.2	1500–3000	24–32	≥80	Semi-diurnal (3–6)
Cuba	421,538	3.1	1000–1500	24–30	≥80	Semi-diurnal (0.5–1.5)
India	368,276	2.7	1500–3000	25–32	75–85	Diurnal and semi-diurnal (2–6)
Guinea Bissau	338,652	2.5	1200–2000	25–32	70–80	Semi-diurnal (2–3)
Mozambique	318,652	2.3	1000–1500	25–30	70–80	Intertidal (1.5–3)
Madagascar	278,078	2.0	800–1500	25–30	≥80	Semi-diurnal (1.5–4)
Philippines	263,137	1.9	1500–3000	25–32	80–90	Intertidal (1–2)

#### 145 **4 Mangrove Area Mapping and Classification**

146 The integration of satellite imagery with geospatial analysis has significantly  
 147 improved the ability of researchers to detect changes in mangrove cover, evaluate  
 148 species distribution, identify areas under ecological stresses, and distinguish man-  
 149 groves from adjacent land cover types such as agricultural fields, mudflats, and  
 150 inland vegetation (Kuenzer et al., 2011). Challenges in mangrove classification  
 151 arose due to similar reflectance from other vegetation, rice fields, and water bodies.  
 152 To overcome this, masking techniques can be used to separate mangrove areas from  
 153 non-mangrove vegetation and water bodies, thus improving the accuracy of the  
 154 classification (Salam et al., 2007). The unsupervised classification using 30 clusters  
 155 in a study yielded an overall accuracy of 78.32% while supervised classification,

supported by 272 ground-truth points, performed better with 81.62% accuracy. In the former method, the water bodies were classified accurately, but misclassifications occurred in identifying species like Gewa and grassland/bare land areas. Some of the classification errors in both methods could be attributed to environmental differences and a time gap between the acquisition of the satellite images and the creation of the mangrove inventory map. Despite this, both methods were considered reliable, with supervised classification slightly outperforming the unsupervised approach. However, some researchers reported that the use of machine learning algorithms such as Support Vector Machines (SVMs) and Random Forest (RF) has even been better to classify mangrove species and mapping and monitoring of mangrove forests (Campomanes et al., 2016; Jiang et al., 2021). The overall accuracy of RF can be 99.17%, whereas SVM showed 95.83% accuracy. Thus, these algorithms can be used for mapping and classification of mangrove ecosystems all over the world.

Numerous researchers used remote sensing techniques for mapping of Indian Sundarbans region (Biswas et al., 2024; Mondal & Bandyopadhyay, 2014; Mitra & Karmaker, 2010; Giri et al., 2007). Net erosion of approximately 3.7 km<sup>2</sup> per year across the Indian Sundarbans Delta between 1980 and 2021, with 243 km<sup>2</sup> of erosion and 91 km<sup>2</sup> of accretion over a 41-year period, was estimated using the NDVI (Biswas et al., 2024). Ghosh et al. (2015) employed an unsupervised (ISODATA) classification on a multi-temporal and multiscale analysis mapping colonial-era charts alongside 1960s Corona imagery and Landsat satellite data and found that the overall mangrove area in the Indian Sundarbans system remained relatively constant over time and there were significant internal changes in forest condition and stand structure, reflecting shifts in density and health of mangrove species. Giri et al. (2007) conducted a multi-temporal Landsat analysis from the 1970s to 2000s and reported that mangrove forest area in the Sundarbans decreased by approximately 1.2% over that period, with a more pronounced decline of approximately 2.5% between 1990s and 2000s. In another study, Datta and Deb (2012) employed multi-temporal Landsat data to investigate on land use/land cover (LULC) changes between 1975 and 2006 revealing a substantial decline of around 0.42% of the area's initial mangrove cover, primarily in the Sundarbans' forest-habitation interference zones. Kundu et al. (2021) classified Landsat imagery using NDVI from 1975 to 2018 into dense forest, sparse forest, water bodies, and wetland and found a net loss of approximately 2.1% ( $\approx 47$  km<sup>2</sup>) of forest area, with varying trends in fragmentation and density. Mondal et al. (2018) used Landsat MSS and OLI multi-spectral satellite imagery to classify land use/land cover (LULC) on Sagar Island into categories such as forest vegetation, agriculture, built-up area, water bodies, and wetlands. Their classification achieved an overall accuracy of 79.53%, with a Kappa coefficient (*K*) of 0.7465.

#### 196 4.1 Change Detection of Mangrove

197 The decrease in mangrove cover and its density is a threat to its flora and fauna. The  
198 monitoring of change in mangrove cover can be performed by adapting various  
199 change detection methods of the remote sensing (RS) technique. The traditional  
200 change detection methods like post-classification comparison (PCC), unsupervised  
201 conventional change detection, change vector analysis (CVA), and single threshold  
202 algorithm (STA) had limitations. To overcome this, Shimu et al. (2019) proposed a  
203 new method of using the Normalized Difference Vegetation Index (NDVI) to track  
204 changes in vegetation over a temporal scale, resulting in both progressive and  
205 regressive changes in mangrove vegetation.

206 The land use/land cover (LULC) change study in the South-Western Indian  
207 Sundarbans Biosphere Reserve from 1975 to 2006 using Landsat imagery showed a  
208 significant loss of open mangrove areas and biodiversity, particularly in forest-  
209 habitation zones, while dense mangrove cover increased in the reserved forests,  
210 indicating effective management (Datta & Deb, 2012). The study also showed that  
211 overall, the region lost about 0.42% of its original mangrove cover, and the rise of  
212 nonagricultural lands is linked to the growth of settlements, tourism, and alternative  
213 livelihoods like shrimp farming and commercial fishing, although harmful practices  
214 like prawn seed collection persisted.

215 Recent advances in remote sensing technologies have greatly improved LULC  
216 change mapping, particularly for mangrove ecosystems. High-resolution satellite  
217 images from sensors such as Sentinel and Landsat have enabled precise and accu-  
218 rate mapping of changes in mangrove cover over time (Kuenzer et al., 2011; Parida  
219 & Kumar, 2020). Samanta and Hazra (2016) employed a hybrid classification  
220 approach using Landsat TM/ETM+ imagery from 1986, 1996, 2002, and 2012 to  
221 assess mangrove cover changes in the Indian Sundarbans. By using the hybrid  
222 approach in combination of unsupervised (ISODATA) and supervised (Maximum  
223 Likelihood Classifier) classification techniques, they were able to classify the man-  
224 grove area into six land cover classes like dense forest, degraded forest, saline  
225 blanks, water body, sand (beaches/dunes), and mud flats. They obtained the classi-  
226 fication accuracies between 85 and 90% and Kappa values of 0.79–0.88. Changes  
227 were analysed using post-classification comparison, highlighting spatial and tempo-  
228 ral patterns of mangrove degradation and conversion, particularly in forest-habita-  
229 tion interference zones. Kumar et al. (2019) used five vegetation indices, viz.  
230 Mangrove Probability Vegetation Index (MPVI), Normalized Difference Wetland  
231 Vegetation Index (NDWVI), Shortwave Infrared Absorption Depth (SIAD),  
232 Normalized Difference Infrared Index (NDII) and Atmospherically Resistant  
233 Vegetation Index (ARVI) in the decision tree algorithm to improve the separability  
234 of mangrove forests from adjacent land cover classes, especially terrestrial vegeta-  
235 tion using Support Vector Machine (SVM), Minimum Distance (MD), and Spectral  
236 Angle Mapper (SAM) and found that SVM performed better than MD and SAM  
237 with an overall precision of 99.08% over the Indian Sundarbans.

The impact analysis of LULC changes is essential for prioritizing the management practices. Thakur et al. (2021) analysed the impact of LULC changes in the Indian Sundarbans from 2000, 2010, and 2017, using Landsat TM, ETM+, and OLI imagery, and found a decline in mangrove swamps, plantations, and agricultural land, while sand beaches, mudflats, rivers, and agriculture increased. NDVI values dropped for mangroves from 0.441 to 0.229 and plantations from 0.266 to 0.195 but rose for rivers and aquaculture. Land Surface Temperature (LST) increased in settlements and sand beaches, showing a negative correlation with NDVI, likely due to the high evapotranspiration of mangroves. The results indicated the growth of non-vegetated areas and ecosystem stress. Similar results were reported by Kanjin and Alam (2024) where they showed changes in mangrove coverage from 1973 to 2023 using Landsat (Landsat 1–8) data and examined the relationship between vegetation health with NDVI and surface temperature using Moderate Resolution Imaging Spectroradiometer (MODIS) data in Bangladesh and Indian Sundarbans. Despite mangrove loss, vegetation health improved, indicating resilience. The study found a weak negative correlation between NDVI and LST, suggesting other factors, such as water bodies and land cover heterogeneity, also influenced temperature. The findings highlighted the need for conservation to prevent further degradation.

## 4.2 Disaster Mapping in Mangrove

Disasters are increasingly threatening populations and affecting sustainable development in the mangrove region. Satellite and unmanned aerial vehicle (UAV) technologies play a key role in disaster management by aiding in preparedness, warning, and response. However, challenges like limited access to high-resolution data and technological gaps remain, particularly between developed and developing countries. Recent advancements, including new spatiotemporal data sources and improved resolutions, offer different kind of solutions (Bello & Aina, 2014). SERVIR-Mekong initiative, in collaboration with NASA and USAID, is one such effort for disaster management carried out with the help of the Asian Disaster Preparedness Center and various regional partners in Cambodia, Laos, Thailand, Myanmar, and Vietnam (SERVIR Global, 2023). It plays a crucial role by offering free access to satellite data, dashboards, and customized decision-support tools designed for flood mapping, early warning systems, and monitoring of the mangrove ecosystem. By linking global data resources with local engagement and training, this showcases how countries can work together to fill gaps in data and capacity. This type of initiative empowers vulnerable coastal communities to manage disaster risks more effectively and boost their environmental resilience (SEI, 2023).

The entire global mangrove ecosystems, including the Indian Sundarbans, are exposed to various disasters like cyclones, hurricanes, typhoons, tsunamis and storm surges, flood inundation, embankment breaching, and coastal erosion (IUCN, 2025; Ghosh & Mistri, 2022). These disasters result severe ecological damage, which can be estimated by using Moderate Resolution Imaging Spectroradiometer

279 (MODIS) Global Disturbance Index (MGDI) given by Mildrexler et al. in 2009. For  
280 monitoring and management of cyclonic disasters, the MGDI was used by Dutta  
281 et al. (2015) in the Indian Sundarbans and found that the mangrove landmass  
282 decreased by approximately 329.45 km<sup>2</sup> at a rate of 7.48 km<sup>2</sup> per year from 1973 to  
283 2017. Mandal et al. (2022) implemented the Analytic Hierarchy Process (AHP)  
284 along with Random Forest (RF) and Artificial Neural Network (ANN) to map multi-  
285 hazard risk of the Sundarbans. Their results showed that the southern and eastern  
286 parts of the study area faced high to extremely high risk, primarily driven by cyclonic  
287 hazards and embankment breaching.

## 288 **5 Degradation and Deforestation of Mangroves**

289 The degradation of mangroves is caused by multiple factors such as sea-level rise,  
290 development of fisheries, hyper-salinity, sediment movement, storm effects, shore-  
291 line erosion, and expansion of eutrophication in the surface depressions of swampy  
292 areas (Paul et al., 2017). About 40% of the tropical and 10.5% of the Sundarbans  
293 mangroves have been lost due to induced sea-level rise, extreme weather events, and  
294 human interferences (Padhy et al., 2022; Ghosh et al., 2015). Anthropogenic factors  
295 influencing the ecosystem have indicated that human-wildlife conflict (24.4%) was  
296 considered the biggest threat, followed by climate change (19.9%), salinity change  
297 (18.8%), livelihood pressures on natural resources (16.6%), shrimp seed collection  
298 (11.5%), and environment and water pollution (8.8%) (Vyas & Sengupta, 2012).

299 Integrating spectral data with other spatial datasets can improve insights, and  
300 documenting the accuracy of the results helps users assess the reliability of the find-  
301 ings (Coops et al., 2006). Landsat satellite data, particularly the Tasseled Cap (TC)  
302 transformation, is widely used for detecting forest disturbances. This study tested  
303 four TC-based data structures, such as brightness, greenness, wetness, and a novel  
304 Disturbance Index (DI), to identify stand-replacing disturbances in Russia and  
305 Washington State, USA. The TC transformations generally outperformed the origi-  
306 nal Landsat reflectance data in detecting changes. DI performed best where distur-  
307 bances are more persistent than the areas where disturbances are more transient.  
308 The study highlights that both local forest recovery rates and the time interval  
309 between Landsat acquisitions should be considered when selecting a Tasseled Cap  
310 (TC) transformation for effective disturbance detection (Healey et al., 2005).

311 The MODIS Global Disturbance Index (MGDI) algorithm, which uses  
312 Aqua/MODIS data (LST and EVI), maps large-scale ecosystem disturbances  
313 (LSEDs) and their impact on the global carbon cycle. The algorithm detects changes  
314 in land-surface energy by analysing annual LST composites, minimizing natural  
315 variability. Applied to North America's woody ecosystems in 2005 and 2006, MGDI  
316 accurately identified wildfires, hurricane windfalls, and logging activities. The anal-  
317 ysis found that 1.5% of North America's woody ecosystems were disturbed in 2005  
318 and 0.5% in 2006, with results consistent with wildfire statistics (Mildrexler et al.,  
319 2009). Deforestation and forest degradation, driven by anthropogenic stress, climate

change, and land conversion, were assessed in the Shendurney Wildlife Sanctuary, Kerala, through GIS, remote sensing, fragstat methods, and NDVI to evaluate forest degradation with spatial and nonspatial data, including anthropogenic and climate data. The disturbance index, ranging from 2.5 to 7.5, was categorized into four disturbance zones, viz. low, medium, high, and very high. This analysis supported the development of forest conservation and management strategies (Jose et al., 2011). These indices and methods can be used for assessing the mangrove degradation and deforestation globally.

## 6 Cyclonic Hazards in Mangrove

Due to climate change, the frequency and severity of cyclonic hazards have increased in the recent past, thereby significantly damaging the mangrove forest. Rising temperatures and rising sea levels exacerbated the damage, limiting the forest's ability to regenerate and threatening environmental sustainability (Gupta, 2021). The mangrove ecology of the Sundarbans has suffered significant damage due to super cyclones such as SIDR, Rashmi, and Aila, which has been effectively estimated by Dutta et al. (2015) using the MODIS Global Disturbance Index (MGDI). They analysed the pre- and post-cyclonic changes in EVI and LST to derive cyclonic impacts on vegetation greenness and surface temperature. The derived MGDI data were also transformed into percentage changes, and they compared them to pre- and post-cyclonic events to identify the cyclonic disturbance, with a threshold of 11% change from the temporal mean to define 'disturbed pixels'. This method can be useful to identify the cyclonic hazards in the mangrove ecosystem.

Cyclonic hazards generally occur due to the wind gusts, flooding, saltwater intrusion, storm surge, etc. (NOAA, 2023). These hazards in the mangrove have been reported by numerous researchers in the recent past (Mandal & Hosaka, 2020; Prakash et al., 2023; Mondal et al., 2024). Mandal and Hosaka (2020), using the classification and regression tree (CART), supervised classification technique on Landsat images to assess NDVI changes before and after 21 cyclones during 1988–2016 in the Google Earth Engine with 86% accuracy and a kappa coefficient of 0.80. They reported that the cyclone-affected forest area ranged from 0.5% to 24.1%, with the 18 cyclones impacting less than 10%, while the cyclone Sidr (24.1%) and one in 1988 (20.4%) caused the most damage. The cyclonic wind speed showed a significant positive correlation with the forest damage. Computing NDVI and EVI indices from the Landsat imagery, Prakash et al. (2023) found that the Amphan super cyclone caused a significant shift in mangrove cover from dense to sparse (approx. 50.18 km<sup>2</sup>). They also reported that the barren land increased by 50.37% based on Normalized Difference Bareness Index (NDBaI), the water-bodies increased by 5.20% based on Normalized Difference Water Index (NDWI), and salinity increased based on Normalized Difference Salinity Index (NDSI).

Recently, Mondal et al. (2024) generated cyclonic flood-effective zones of the Sundarbans with the flood susceptibility spectral indices such as Normalized

361 Difference Vegetation Index (NDVI), Modified Normalized Difference Water Index  
362 (MNDWI), Normalized Difference Moisture Index (NDMI), Normalized Difference  
363 Built-up Index (NDBI), Bare Soil Index (BSI), and Normalized Difference Turbidity  
364 Index (NDTI) using Landsat 8 Operational Land Imager, Thermal Infrared Sensor,  
365 Resourcesat, LISS-III, and AWiFS sensors data. They found that the riverine and  
366 coastal areas in the northeast and southwest of the Sundarbans were highly suscep-  
367 tible to floods. Among the flood susceptibility indices, the MNDWI was found to be  
368 highly and significantly correlated with Normalized Difference Flood Index (NDFI).

## 369 7 Fire Hazards in Mangroves

370 Mangrove forest fires, though historically rare, have been increasingly recorded  
371 globally, particularly during natural droughts such as El Niño events, which dry out  
372 litter and peat layers, and when coupled with human activities like slash-and-burn  
373 agriculture, land conversion, and waste burning (Dookie et al., 2025). Fire hazards  
374 in mangrove forests are unlikely because of regular water inundation due to two  
375 high tides in a day. The typical swampy nature of the ecosystems is also protecting  
376 it from fire hazards. Extreme heat and high winds, especially during the dry season,  
377 further exacerbate the fire risk in the forests. The man-made fires are often attributed  
378 to discarded cigarettes from fishermen and honey collectors, clearing of paths  
379 through the mangrove forest or the flames from torches used to repel bees.

380 Bangladesh's Sundarbans face frequent fire hazards. Between 1970 and 2024,  
381 the Bangladesh forest department and residents reported a total of 40 fire incidents  
382 in the same area. Fire incidents in Bangladesh's East Sundarbans now occur nearly  
383 every year during the dry season. In many parts of the region, the canals that connect  
384 villages to the Sundarbans have dried up, and during summer, ponds within the  
385 mangroves also dry out. This increasing dryness leaves the forests highly suscepti-  
386 ble to fires, which can spread rapidly due to a lack of manpower in the forest  
387 department.

388 Similar to the Bangladesh Sundarbans, many other mangrove ecosystems of the  
389 world are vulnerable to fire hazards. Remote sensing techniques like the Normalized  
390 Burn Ratio (NBR), Burn Area Index (BAI), and Mid-Infrared Burn Index (MIRBI)  
391 use reflectance differences in MIR and NIR bands to delineate recently burned  
392 regions versus unburned vegetation (Kurbanov et al., 2022). Using multi-temporal  
393 Landsat imagery and Normalized Burn Ratio (NBR) and differenced NBR (dNBR),  
394 a study detected that over 800 hectares of mangroves in South Sumatra experienced  
395 moderate to high burn severity (dNBR values exceeding 0.3) during the 2015 El  
396 Niño-driven fire season, particularly in inland zones, which are less influenced by  
397 tidal flooding (Crowe, 2020). Also, a fuel-type map and forest fire hazard rating for  
398 swampy mangrove forests can be developed using remote sensing data like Landsat  
399 TM imagery. By integrating this data with GIS layers such as fuel type, roads, and  
400 canals, a fire hazard rating map can be created (Razali et al., 2010). Fuzzy set theory  
401 integrated with decision-making algorithms within a GIS framework can be used to

map potential forest fire risk and guide proactive fire management efforts (Vadrevu et al., 2010). However, in contrast to the Bangladesh Sundarbans, the Indian Sundarbans is clearly defined by natural boundaries, which help keep it completely free from encroachment and, thereby, protected from fire hazards. Because of the tidal fluctuations, the entire region is flooded twice daily, preventing any fire outbreaks. Also, due to the terrain, location, and diversity of species, the area is free from grazing activities.

## 8 Biomass Estimation

Accurate estimation of mangrove biomass is important for determining carbon stock, exploring climate mitigation potential, and directing restoration efforts in mangrove ecosystems. Simard et al. (2019) mapped the global mangrove canopy height and biomass estimate using ICESat Geoscience Laser Altimeter System (GLAS) LiDAR data and found a significant correlation between above-ground biomass (AGB) and canopy height. Using this method, the total global mangrove carbon stock (above and below-ground biomass and soil) is estimated at 5.03 Pg. Anand et al. (2020) integrated EO-1 Hyperion hyperspectral data with Bhitarkanika field data to estimate carbon stock and biomass. Ten mangrove species were classified using the SAM classifier with a Kappa value of 0.81. Between different regression models, a second-order polynomial based on EVI provided the greatest accuracy ( $R^2 \approx 0.87$ ), followed by NDVI ( $R^2 \approx 0.84$ ), predicting carbon stocks between 459,820 and 514,470 tonnes.

The multi-temporal Sentinel-1 and 2 data-derived variables were used by Ghosh et al. (2021) to estimate the above-ground biomass (AGB) using variables such as, Normalized Difference Vegetation Index (NDVI), Soil Adjusted Vegetation Index (SAVI), Green NDVI (GNDVI), Normalized Difference Index produced using band 4 and 5 of Sentinel-2 data (NDI45), Inverted Red-Edge Chlorophyll Index (IRCEI), Transformed Normalized Difference Vegetation Index (TNDVI), Enhanced Vegetation Index (EVI), and Two Bands Enhanced Vegetation Index (EVI2) in Bhitarkanika Wildlife Sanctuary by Random Forest (RF), Gradient Boosted Model (GBM), and Extreme Gradient Boosting (XGB) models. The best performance was achieved using an ensemble model with a reduced RMSE of 72.86 t/ha and a normalized RMSE of 11.38% which implies that ensemble machine learning techniques enhance the precision of biomass estimation in mangrove ecosystems and support improved blue carbon assessments. In 2017, Castillo et al. estimated and mapped above-ground biomass (AGB) of mangrove forests using a combination of satellite-derived predictors that included SAR backscatter coefficients (VH and VV), GLCM texture features, and vegetation indices such as NDVI and EVI from Sentinel-2. The resulting biomass maps achieved overall accuracy between 85.3 and 86.6% with RMSE values between 27.8 and 28.5 Mg/ha and correlation coefficients ( $r$ ) ranging from 0.82 to 0.84, demonstrating potential for scalable blue carbon stock assessments and land-use change monitoring.

443 By using image processing and digital photogrammetry, a canopy height model  
444 (CHM) generated using drone-based RGB images could reliably estimate tree  
445 height, offering an efficient method for forest inventory. This approach has the  
446 potential to enhance forest management across various land tenures and forest types  
447 (Srivastava et al., 2022). UAV-based photogrammetry combined with allometric  
448 equations improved the accuracy for estimation of above-ground biomass in both  
449 natural and restored mangrove ecosystems using digital surface models (DSM) and  
450 digital terrain models (DTM) to generate canopy height models (CHMs). The mean  
451 total AGB in natural mangroves and restored mangroves was found to be 239 Mg/  
452 ha and 232 Mg/ha, respectively (Basyuni et al., 2025). Overall, these methods provide  
453 non-destructive, scalable, and economical biomass assessment techniques that  
454 are crucial for ecosystem monitoring, blue carbon accounting, and climate mitigation  
455 plans.

## 456 9 Species Discrimination in Mangrove

457 Accurate monitoring of mangrove species distribution is vital for assessing their  
458 health and supporting restoration efforts due to their enormous ecological and economic  
459 importance. Hyperspectral sensors could aid species identification, though  
460 field challenges may arise (Vaiphasa et al., 2005). Spectral data (2151 bands between  
461 350 and 2500 nm) of crown canopy leaves from 16 Thai mangrove species were  
462 captured under laboratory conditions and tested statistically to assess species differentiation.  
463 Significant differences were found in 1941 bands ( $p < 0.05$ ), with 477  
464 bands at  $p < 0.01$ . Spectral separability, measured by the Jeffries-Matusita distance,  
465 showed most species could be separated, except for those in the Rhizophoraceae  
466 family. Using high-resolution multispectral remote sensing images, the location of  
467 species, *A. marina*, *A. alba*, and *A. officinalis* along the gradients of soil salinity  
468 were identified by Mitra and Karmaker (2010) having ecological optima at salinity  
469 values of 18.2 and 20.1 ppt, 17.5 and 18.6 ppt, and 13.02 and 25 ppt, respectively,  
470 indicating *A. marina* as the most salt-tolerant mangrove species in the Indian  
471 Sundarbans. Giri et al. (2014) employed Landsat TM and ETM+ images from 2010  
472 and 1999, respectively, to detect changes in particular mangrove species zones,  
473 revealing that *Avicennia* sp. is the most dominant species, followed by *Excoecaria*  
474 sp. and *Phoenix* sp. Using Landsat satellite series images, Ghosh et al. (2016) were  
475 able to identify mangrove species composition and detect species-level over time,  
476 showing that *H. fomes* and *E. agallocha* both decreased by 9.9% in the Indian  
477 Sundarbans, while *Ceriops decandra*, *Sonneratia apetalata*, and *Xylocarpus mekongensis*  
478 increased by 12.9%, 38.4% and 57.3%, respectively.

479 Recently, a framework was developed using multisource spaceborne high-  
480 resolution imagery such as WorldView-2 (WV-2), Orbital HyperSpectral (OHS),  
481 and Advanced Land Observing Satellite-2 (ALOS-2) to classify mangrove species  
482 at a finer scale. Key variables for species classification were identified through the  
483 application of extreme gradient boosting with recursive feature elimination

(XGBoost-RFE) (Zhen et al., 2024). Anand et al. (2020) utilized Hyperion EO-1 hyperspectral satellite data (220 bands) to map dominant species in the Bhitarkanika mangroves through spectral angle mapping (SAM) and partial least squares regression (PLSR). According to the study, *Avicennia marina* had stronger reflectance in SWIR region because of leaf salt excretion, whereas *Rhizophora mucronata* had strong absorption in the NIR region because of its denser canopy structure and indicated overall classification accuracies of 80–85%.

## 10 Sundarbans Mangrove of India: A Case Study

The Indian Sundarbans, recognised as a World Heritage Site by UNESCO, is a biodiversity hotspot and a unique ecosystem by being the world's largest continuous mangrove ecosystem. This ecosystem plays a key role both ecologically and economically by protecting the area from cyclone-driven coastal erosion and for people's livelihoods by providing resources such as honey, fuelwood, and fish. The climate of the Sundarbans is subtropical. Temperature changes from 20 °C in December–January to 28 °C in June–July. The annual average rainfall is around 1963 mm, 75% of which occurs during June to September. This is in a tropical cyclone belt and often demonstrates a complex interaction between social and ecological systems.

The fluctuating water levels, temperature, and wind flow are affecting the topography of the area, making it prone to several natural hazards, leading to the destruction of forest resources, especially under climate change scenarios. The Sundarbans faces severe climate change challenges, including rising sea levels, increasing salinity, and frequent cyclones, which threaten both its ecosystem and local livelihoods. Some urgent actions, such as global emission reductions, promoting saline-resistant plants, and improving disaster response, are needed to protect the region from further damage and potential submergence (Mahadevia Ghimire & Vikas, 2012). Native mangrove species like *Avicennia marina*, *Rhizophora mucronata*, *Sonneratia apetala*, and *Ceriops decandra* are recognized for their high resistance to salt, ability to adapt to changing water conditions, and importance in stabilizing soil and supporting biodiversity. *Avicennia marina* can tolerate salinity levels over 60 parts per thousand (Parida & Jha, 2010). The forest area of the Sundarbans region is divided into two broad categories: (1) saltwater heritiera and (2) low mangrove. A large part of the 'reserve' forest areas known as 'tiger reserves' has been declared 'totally protected', and no forestry operation is allowed there. The most noted species of the wildlife of the region are the royal Bengal tiger, spotted deer, wild boar, and crocodiles.

The anthropogenic interference in the Sundarbans began in the late eighteenth century mainly through agricultural practices. The deforestation contributes 6–17% of anthropogenic CO<sub>2</sub> emission, for example, from 2000 to 2010, about 1.0 Pg C/year was emitted (Baccini et al., 2012). Further, the encroachment of seawater into the mangrove increases salinity, resulting in loss of high-value storm-stopping tree

525 species such as Sundari (*Heritiera littoralis*), which gives this area the name  
526 Sundarbans. This is further affected by reduced freshwater and sediment supply to  
527 the system due to upstream dams on the rivers. There are many indicators of such  
528 deleterious effects, e.g. few mangrove islands have vanished over the last century,  
529 some have significantly shrunk over the last 50 years, houses are swept away due to  
530 repeated collapse of river embankments, abandoning rice farming for shrimping,  
531 and increased incidence of water-borne diseases. A comparison of the area with  
532 earlier survey records (e.g. early nineteenth-century Dampier and Hodges survey of  
533 forest extent) indicates that the mangrove has shrunk to almost half in size.

534 India's current mangrove cover is 4991.68 km<sup>2</sup>, or 0.15% of its entire geographical  
535 area. According to the Forest Survey of India, the mangrove cover is categorized  
536 into Very Dense (canopy density of 70% and above), Moderately Dense (canopy  
537 density of 40% and more but less than 70%) and Open categories (canopy density  
538 of 10% and more but less than 40%). Very Dense Mangroves encompass 1463.97 km<sup>2</sup>  
539 (29.33% of the total mangrove area); Moderately Dense Mangroves cover  
540 1500.81 km<sup>2</sup> (30.07%); and Open Mangroves cover 2026.87 km<sup>2</sup> (40.60%). India's  
541 mangrove cover has decreased from 2021 to 2023 by a net 7.43 km<sup>2</sup>. The highest  
542 mangrove cover is found in the Sundarbans region of West Bengal (42.5% of the  
543 India's total mangrove cover) followed by Gujarat (23.3%), Andhra Pradesh (8.4%),  
544 Maharashtra (6.3%), and Odisha (5.2%). West Bengal has the largest expanse of  
545 extremely dense mangroves, covering about 981.63 km<sup>2</sup> out of the total mangrove  
546 area of 2119.16 km<sup>2</sup> followed by Gujarat, which contains 1164.06 km<sup>2</sup> of mangrove  
547 cover, predominantly featuring open mangroves (Table 3). The lowest mangrove  
548 cover is found in the Karaikal District of Puducherry. The states that show signifi-  
549 cant gain in mangrove cover are Andhra Pradesh (13 km<sup>2</sup>) and Maharashtra (12 km<sup>2</sup>).  
550 The rise in mangrove cover in Andhra Pradesh is mostly due to natural regeneration  
551 and plantation initiatives, conservation efforts and addition of leftover patches.  
552 Andhra Pradesh's districts of Krishna, Bapatla, and Kakinada have all seen a rise. In  
553 Maharashtra, the increase in mangrove cover is mostly attributable to natural regen-  
554 eration and plantations done by the State government. The growth in mangrove  
555 cover has been found in the Raigarh and Palghar districts of Maharashtra. But there  
556 is a prominent decrease in mangrove cover observed in Gujarat by 36 km<sup>2</sup> (India  
557 State of Forest Report, Vol. 1, 2023).

558 The Land Use Land Cover (LULC) analysis and mapping of the Sundarbans  
559 region of the state of West Bengal in India were carried out to provide information  
560 to help users understand the problems and prospects of the unique ecosystem. The  
561 Landsat data for the years 1988 and 2022 were used for LULC classification using  
562 supervised classification in the QGIS environment (Fig. 2). The Sundarbans region  
563 was classified into seven LULC classes, such as forest, vegetation, river, water body,  
564 fallow land, agricultural land, and built-up areas for both years using a supervised  
565 classification method. The respective changes of these classes were -313.8, +139.0,  
566 -102.4, +259.0, +625.8, -1465.9, and +858.2 km<sup>2</sup>. The positive sign (+) denoted  
567 the increase of the area under a particular class, and the negative sign (-) denoted  
568 its decrease in the year of 2022 from 1988. Over 34 years of time, the lands under  
569 the forest, river, and agriculture classes have decreased substantially. However, the

**Table 3** State/Union Territories (UT)-wise Mangrove Cover Assessment 2023 (in km<sup>2</sup>) in India

Sl. no.	State/UT	Very dense mangrove	Moderately dense mangrove	Open mangrove	Total mangrove cover
1	Andhra Pradesh	0.00	213.90	207.53	421.43
2	Goa	0.00	23.75	7.59	31.34
3	Gujarat	0.00	179.09	984.97	1164.06
4	Karnataka	0.11	3.15	10.94	14.20
5	Kerala	0.00	4.73	4.72	9.45
6	Maharashtra	0.00	89.82	225.27	315.09
7	Odisha	81.67	94.61	82.78	259.06
8	Tamil Nadu	1.19	25.07	15.65	41.91
9	West Bengal	981.63	703.79	433.74	2119.16
10	A & N Islands	399.37	162.64	46.28	608.29
11	D& NH and Daman & Diu	0.00	0.21	3.65	3.86
12	Puducherry	0.00	0.08	3.75	3.83
<b>Total</b>		<b>1463.97</b>	<b>1500.94</b>	<b>2046.87</b>	<b>5011.78</b>

Source: India's Biennial State of Forest Report, 2023

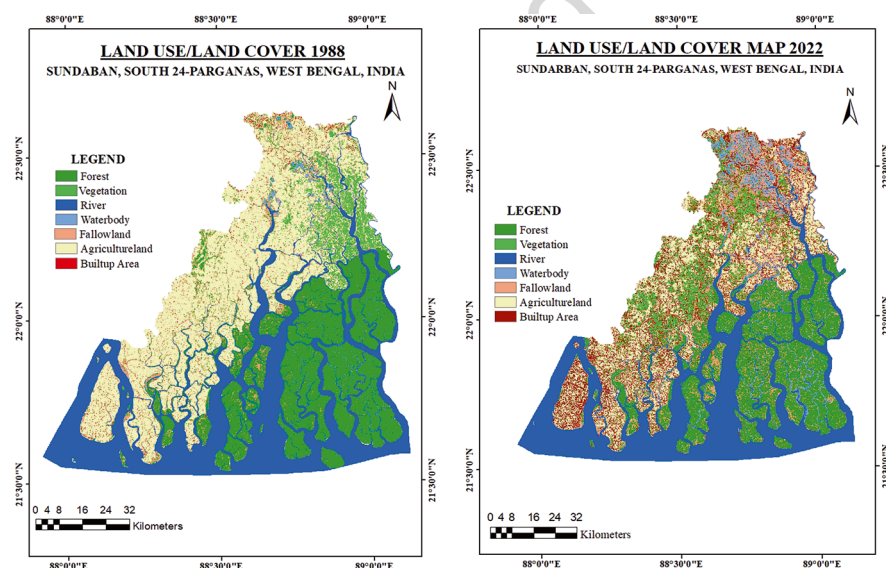


**Fig. 2** Land use land cover map of the Indian Sundarbans region for the years 1988 and 2022

lands under other vegetation, water bodies (other than rivers), fallow, and built-up areas have increased in the Sundarbans region. This LULC mapping will enable the monitoring of temporal dynamics of agricultural ecosystems, forest conversions, surface water bodies, etc. on a timely basis for fulfilling the sustainable development goal in the Indian Sundarbans region.

570  
571  
572  
573  
574

## 575 11 Future Need for Remote Sensing Research on Mangrove

576 Mangrove forests are threatened by many human pressures, including conversion to  
 577 aquaculture and agriculture, coastal development, overharvesting, agricultural and  
 578 industrial pollutions, and climate change impacts. There is an urgent need for  
 579 homogenized classification schemes and standardized data-processing methods for  
 580 remote sensing-based assessment of mangrove ecosystems using common plat-  
 581 forms like Google Earth Engine, Copernicus Global Land Services, etc. This will  
 582 enable a coherent and seamless data accessibility to the next users for generating the  
 583 new comparable data with the archive. Similarly, a homogenized transparent accu-  
 584 racy assessment will give confidence for prioritizing the issues. This can provide  
 585 insights into researchable issues and the adoption of new techniques for the man-  
 586 grove ecosystems. Developing a database management system for the world man-  
 587 grove will promote further investigations on synergetic data use. Satellite and  
 588 unmanned aerial vehicle (UAV) can play a major role in the evaluation of ecosystem  
 589 services of mangrove by interdisciplinary and well-networked research teams at the  
 590 regional, national, and global level.

591 **Acknowledgements** This chapter is an outcome of the Multinational Collaborative Project par-  
 592 tially supported by Asia Pacific Network for Global Change Research (APN-GCR) and University  
 593 of the Sunshine Coast (UniSC), Australia. The logistic support from the Indian Council of  
 594 Agricultural Research for the study is duly acknowledged.

## 595 References

- 596 Anand, A., Pandey, P. C., Petropoulos, G. P., Pavlides, A., Srivastava, P. K., Sharma, J. K., & Malhi,  
 597 R. K. M. (2020). Use of hyperion for mangrove forest carbon stock assessment in Bhitarkanika  
 598 forest reserve: A contribution towards blue carbon initiative. *Remote Sensing*, *12*(4), 597.
- 599 Baccini, A. G. S. J., Goetz, S. J., Walker, W. S., Laporte, N. T., Sun, M., Sulla-Menashe, D.,  
 600 Hackler, J., Beck, P. S. A., Dubayah, R., Friedl, M. A., & Samanta, S. (2012). Estimated car-  
 601 bon dioxide emissions from tropical deforestation improved by carbon-density maps. *Nature*  
 602 *Climate Change*, *2*(3), 182–185.
- 603 Baccini, A., Walker, W., Carvalho, L., Farina, M., Sulla-Menashe, D., & Houghton, R. A. (2017).  
 604 Tropical forests are a net carbon source based on aboveground measurements of gain and loss.  
 605 *Science*, *358*(6360), 230–234.
- 606 Barbier, E. B., Hacker, S. D., Kennedy, C., Koch, E. W., Stier, A. C., & Silliman, B. R. (2011). The  
 607 value of estuarine and coastal ecosystem services. *Ecological Monographs*, *81*(2), 169–193.
- 608 Basyuni, M., Mubaraq, A., Amelia, R., Wirasatriya, A., Iryanthony, S. B., Slamet, B., Al Mustaniroh,  
 609 S. S., Pradisty, N. A., Sidik, F., Hanintyo, R., & Sumarga, E. (2025). Mangrove aboveground  
 610 biomass estimation using UAV imagery and a constructed height model in Budeng–Perancak,  
 611 Bali, Indonesia. *Ecological Informatics*, *86*, 103037.
- 612 Bello, O. M., & Aina, Y. A. (2014). Satellite remote sensing as a tool in disaster management  
 613 and sustainable development: Towards a synergetic approach. *Procedia-Social and Behavioral*  
 614 *Sciences*, *120*, 365–373.

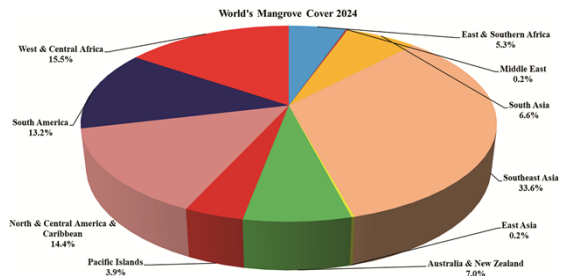
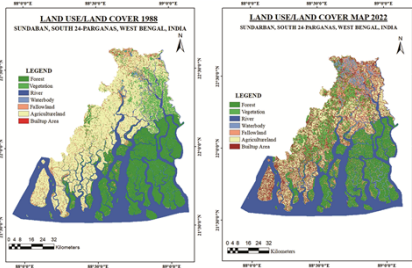
- Biswas, S., Sarkar, K., & Das, T. K. (2024). Decadal changes (1980–2021) of shoreline and mangrove cover in Sundarban Delta, India, using remote sensing and GIS. *Journal of Physical Oceanography*, 54(8), 1655–1674. 615  
616  
617
- Campomanes, F., Pada, A. V., & Silapan, J. (2016, September). Mangrove classification using support vector machines and random forest algorithm: A comparative study. In *6th International Conference on Geographic Object-Based Image Analysis, GEOBIA 2016: Solutions & Synergies*. University of Twente, Faculty of Geo-Information Science and Earth Observation (ITC). 618  
619  
620  
621  
622
- Castillo, J. A. A., Apan, A. A., Maraseni, T. N., & Salmo, S. G., III. (2017). Estimation and mapping of above-ground biomass of mangrove forests and their replacement land uses in the Philippines using Sentinel imagery. *ISPRS Journal of Photogrammetry and Remote Sensing*, 134, 70–85. 623  
624  
625  
626
- Chapman, V. J. (1976). Mangrove vegetation. J. Cramer, Vaduz, Pp. 447. 627
- Church, J. A., & White, N. J. (2011). Sea-level rise from the late 19th to the early 21st century. *Surveys in Geophysics*, 32(4), 585–602. 628  
629
- Clark, D. A., Piper, S. C., Keeling, C. D., & Clark, D. B. (2003). Tropical rain forest tree growth and atmospheric carbon dynamics linked to interannual temperature variation during 1984–2000. *Proceedings of the National Academy of Sciences*, 100(10), 5852–5857. 630  
631  
632
- Coops, N. C., Wulder, M. A., & White, J. C. (2006). Identifying and describing forest disturbance and spatial pattern: Data selection issues and methodological implications. In *Forest disturbance and spatial pattern: Remote sensing and GIS approaches* (p. 264). 633  
634  
635
- Crowe, M. (2020). Do mangroves burn? A remote sensed study of the impacts of forest fires on mangrove populations in South Sumatra, Indonesia. MSc degree in Climate Change Science and Policy, King's College London. 636  
637  
638
- Datta, D., & Deb, S. (2012). Analysis of coastal land use/land cover changes in the Indian Sunderbans using remotely sensed data. *Geo-spatial Information Science*, 15(4), 241–250. 639  
640
- Dookie, S., Ansari, A. A., & Jaikishun, S. (2025). Forest-fire interactions, impacts, and implications: A focus on mangroves. *New Zealand Journal of Forestry Science*, 55. 641  
642
- Duke, N., Ball, M., & Ellison, J. (1998). Factors influencing biodiversity and distributional gradients in mangroves. *Global Ecology & Biogeography Letters*, 7(1), 27–47. 643  
644
- Dutta, D., Das, P. K., Paul, S., Sharma, J. R., & Dadhwal, V. K. (2015). Assessment of ecological disturbance in the mangrove forest of Sunderbans caused by cyclones using MODIS time-series data (2001–2011). *Natural Hazards*, 79(2), 775–790. 645  
646  
647
- FAO, 2020. Global Forest Resources Assessment 2020: Main report. . 648
- Ganguly, S., Nemani, R. R., Zhang, G., Hashimoto, H., Milesi, C., Michaelis, A., Wang, W., Votava, P., Samanta, A., Melton, F., & Dungan, J. L. (2012). Generating global leaf area index from Landsat: Algorithm formulation and demonstration. *Remote Sensing of Environment*, 122, 185–202. 649  
650  
651  
652
- Ghosh, S., & Mistri, B. (2022). Analyzing the multi-hazard coastal vulnerability of Matla–Bidya inter-estuarine area of Indian Sunderbans using analytical hierarchy process and geospatial techniques. *Estuarine, Coastal and Shelf Science*, 279, 108144. 653  
654  
655
- Ghosh, A., Schmidt, S., Fickert, T., & Nüsser, M. (2015). The Indian Sundarban mangrove forests: History, utilization, conservation strategies and local perception. *Diversity*, 7(2), 149–169. 656  
657
- Ghosh, M. K., Kumar, L., & Roy, C. (2016). Mapping long-term changes in mangrove species composition and distribution in the Sunderbans. *Forests*, 7(12), 305. 658  
659
- Ghosh, S. M., Behera, M. D., Jagadish, B., Das, A. K., & Mishra, D. R. (2021). A novel approach for estimation of aboveground biomass of a carbon-rich mangrove site in India. *Journal of Environmental Management*, 292, 112816. 660  
661  
662
- Gilman, E. L., Ellison, J., Duke, N. C., & Field, C. (2008). Threats to mangroves from climate change and adaptation options: A review. *Aquatic Botany*, 89(2), 237–250. 663  
664
- Giri, C., Pengra, B., Zhu, Z., Singh, A., & Tieszen, L. L. (2007). Monitoring mangrove forest dynamics of the Sunderbans in Bangladesh and India using multi-temporal satellite data from 1973 to 2000. *Estuarine, Coastal and Shelf Science*, 73(1–2), 91–100. 665  
666  
667

- 668 Giri, S., Mukhopadhyay, A., Hazra, S., Mukherjee, S., Roy, D., Ghosh, S., Ghosh, T., & Mitra,  
669 D. (2014). A study on abundance and distribution of mangrove species in Indian Sundarban  
670 using remote sensing technique. *Journal of Coastal Conservation*, 18(4), 359–367.
- 671 Global Mangrove Watch. (2020). *Mangrove extent dataset*. <https://www.globalmangrovetwatch.org>
- 672 Gupta, S. (2021). Disturbance of mangrove forest due to climate change: The prospects of  
673 Sundarban. *International Journal of Multidisciplinary: Applied Business and Education*  
674 *Research*, 2(12), 1306–1313.
- 675 He, B., Lai, T., Fan, H., Wang, W., & Zheng, H. (2007). Comparison of flooding-tolerance in  
676 four mangrove species in a diurnal tidal zone in the Beibu Gulf. *Estuarine, Coastal and Shelf*  
677 *Science*, 74(1–2), 254–262.
- 678 Healey, S. P., Cohen, W. B., Zhiqiang, Y., & Krankina, O. N. (2005). Comparison of Tasseled  
679 Cap-based Landsat data structures for use in forest disturbance detection. *Remote Sensing of*  
680 *Environment*, 97(3), 301–310.
- 681 IPCC. (2013). Summary for policymakers. In T. F. Stocker, D. Qin, G.-K. Plattner, M. Tignor,  
682 S. K. Allen, J. Boschung, A. Nauels, Y. Xia, V. Bex, & P. M. Midgley (Eds.), *Climate change*  
683 *2013: The physical science basis. Contribution of Working Group I to the Fifth Assessment*  
684 *Report of the Intergovernmental Panel on Climate Change*. Cambridge University Press.
- 685 Iqbal, M. H. (2020). Valuing ecosystem services of Sundarbans Mangrove Forest: Approach of  
686 choice experiment. *Global Ecology and Conservation*, 24, e01273.
- 687 IUCN. (2025). *The IUCN red list of threatened species*. Version 2025-1. Retrieved July 28, 2025.
- 688 Jiang, Y., Zhang, L., Yan, M., Qi, J., Fu, T., Fan, S., & Chen, B. (2021). High-resolution mangrove  
689 forests classification with machine learning using worldview and UAV hyperspectral data.  
690 *Remote Sensing*, 13(8), 1529.
- 691 Jose, S., Alex, C. J. C. J., Kumar, S., Varghese, A., & Madhu, G. (2011). Landscape metric  
692 modeling—A technique for forest disturbance assessment in Shendurney wildlife sanctuary.  
693 *Environmental Research, Engineering and Management*, 58(4), 34–41.
- 694 Kanjin, K., & Alam, B. M. (2024). Assessing changes in land cover, NDVI, and LST in the  
695 Sundarbans mangrove forest in Bangladesh and India: A GIS and remote sensing approach.  
696 *Remote Sensing Applications: Society and Environment*, 36, 101289.
- 697 Kuenzer, C., Bluemel, A., Gebhardt, S., Quoc, T. V., & Dech, S. (2011). Remote sensing of man-  
698 grove ecosystems: A review. *Remote Sensing*, 3(5), 878–928.
- 699 Kumar, T., Mandal, A., Dutta, D., Nagaraja, R., & Dadhwal, V. K. (2019). Discrimination and clas-  
700 sification of mangrove forests using EO-1 Hyperion data: A case study of Indian Sundarbans.  
701 *Geocarto International*, 34(4), 415–442.
- 702 Kundu, K., Halder, P., & Mandal, J. K. (2021). Change detection and patch analysis of Sundarban  
703 forest during 1975–2018 using remote sensing and GIS data. *SN Computer Science*, 2(5), 364.
- 704 Kurbanov, E., Vorobev, O., Lezhnin, S., Sha, J., Wang, J., Li, X., Cole, J., Dergunov, D., & Wang,  
705 Y. (2022). Remote sensing of forest burnt area, burn severity, and post-fire recovery: A review.  
706 *Remote Sensing*, 14(19), 4714.
- 707 Mahadevia Ghimire, K., & Vikas, M. (2012). Climate change–impact on the Sundarbans, a case  
708 study. *International Scientific Journal: Environmental Science*, 2(1), 7–15.
- 709 Mandal, M. S. H., & Hosaka, T. (2020). Assessing cyclone disturbances (1988–2016) in the  
710 Sundarbans mangrove forests using Landsat and Google Earth Engine. *Natural Hazards*,  
711 102(1), 133–150.
- 712 Mandal, P., Maiti, A., Paul, S., Bhattacharya, S., & Paul, S. (2022). Mapping the multi-hazards  
713 risk index for coastal block of Sundarban, India using AHP and machine learning algorithms.  
714 *Tropical Cyclone Research and Review*, 11(4), 225.
- 715 Mildrexler, D. J., Zhao, M., & Running, S. W. (2009). Testing a MODIS global disturbance index  
716 across North America. *Remote Sensing of Environment*, 113(10), 2103–2117.
- 717 Mitra, D., & Karmaker, S. (2010). Mangrove classification in Sundarban using high resolution  
718 multi-spectral remote sensing data and GIS. *Asian Journal of Environment and Disaster*  
719 *Management*, 2(2).

- Mondal, I., & Bandyopadhyay, J. (2014). Coastal zone mapping through geospatial technology for resource management of Indian Sundarban, West Bengal, India. *International Journal of Remote Sensing Applications*, 4(2), 103–112.
- Mondal, I., Thakur, S., Ghosh, P., De, T. K., & Bandyopadhyay, J. (2018). Land use/land cover modeling of Sagar Island, India using remote sensing and GIS techniques. In *Emerging technologies in data mining and information security: Proceedings of IEMIS 2018* (Vol. 1, pp. 771–785). Springer Singapore.
- Mondal, B. K., Mahata, S., Basu, T., Das, R., Patra, R., Abdelrahman, K., Fnais, M. S., & Praharaj, S. (2024). Analysis of the post-cyclonic physical flood susceptibility and changes of mangrove forest area using multi-criteria decision-making process and geospatial analysis in Indian Sundarbans. *Atmosphere*, 15(4), 432.
- Mukherjee, N., Sutherland, W. J., Khan, M. N. I., Berger, U., Schmitz, N., Dahdouh-Guebas, F., & Koedam, N. (2014). Using expert knowledge and modeling to define mangrove composition, functioning, and threats and estimate time frame for recovery. *Ecology and Evolution*, 4(11), 2247–2262.
- Nerem, R. S., Chambers, D. P., Choe, C., & Mitchum, G. T. (2010). Estimating mean sea level change from the TOPEX and Jason altimeter missions. *Marine Geodesy*, 33(S1), 435–446.
- NOAA. (2015). National Oceanic and Atmospheric Administration, National Ocean Service, Center for Operational Oceanographic Products and Services, Tides and Currents. <http://tide-sandcurrents.noaa.gov/>
- NOAA. (2023). *Cyclone hazards & safety*. <https://www.noaa.gov/jetstream/tc-hazards>
- Padhy, S. R., Dash, P. K., & Bhattacharyya, P. (2022). Challenges, opportunities, and climate change adaptation strategies of mangrove-agriculture ecosystem in the Sundarbans, India: A review. *Wetlands Ecology and Management*, 30(1), 191–206.
- Parida, A. K., & Jha, B. (2010). Salt tolerance mechanisms in mangroves: A review. *Trees*, 24(2), 199–217.
- Parida, B. R., & Kumar, P. (2020). Mapping and dynamic analysis of mangrove forest during 2009–2019 using landsat-5 and sentinel-2 satellite data along Odisha Coast. *Tropical Ecology*, 61(4), 538–549.
- Paul, A. K., Ray, R., Kamila, A., & Jana, S. (2017). Mangrove degradation in the Sundarbans. In *Coastal wetlands: Alteration and remediation* (pp. 357–392). Springer International Publishing.
- Prakash, S., Varghese, A., Amrutha, A. S., & Baiju, K. R. (2023). Assessment of ecological disturbance on Indian sundarbans with special reference to Amphan Cyclone by using geospatial technology. *Journal of Geospatial Surveying*, 3(1), 26.
- Randhir, T. O., Toffling, K., & Griffin, C. R. (2024). Impacts of climate change and variability on the growth potential of global mangrove distribution. *Sustainable and Resilient Infrastructure*, 9(1), 63–71.
- Razali, S. M., Nuruddin, A. A., Malek, I. A., & Patah, N. A. (2010). Forest fire hazard rating assessment in peat swamp forest using Landsat thematic mapper image. *Journal of Applied Remote Sensing*, 4(1), 043531.
- Salam, M. A., Ross, L. G., & Beveridge, C. M. C. (2007). The use of GIS and remote sensing techniques to classify the Sundarbans Mangrove vegetation. *Journal of Agroforestry and Environment*, 1(1), 7–15.
- Samanta, K., & Hazra, S. (2016). Mangrove forest cover changes in Indian Sundarban (1986–2012) using remote sensing and GIS. In *Environment and earth observation: Case studies in India* (pp. 97–108). Springer International Publishing.
- SEI (Stockholm Environment Institute). (2023). *NASA data and images help increase climate resilience in the Mekong region*. <https://www.sei.org/features/nasa-data-images-help-increase-climate-resilience-mekong-region/>
- SERVIR Global. (2023). *SERVIR-Mekong*. <https://www.servirglobal.net/Global/Regions/SERVIR-Mekong>
- Shimu, S. A., Aktar, M., Afjal, M. I., Nitu, A. M., Uddin, M. P., & Al Mamun, M. (2019, December). NDVI based change detection in Sundarban Mangrove Forest using remote sensing data. In

- 773       2019 4th International Conference on Electrical Information and Communication Technology  
774       (EICT) (pp. 1–5). IEEE.
- 775 Simard, M., Fatoyinbo, L., Smetanka, C., Rivera-Monroy, V. H., Castañeda-Moya, E., Thomas,  
776       N., & Van der Stocken, T. (2019). Mangrove canopy height globally related to precipitation,  
777       temperature and cyclone frequency. *Nature Geoscience*, *12*(1), 40–45.
- 778 Srivastava, S. K., Seng, K. P., Ang, L. M., Pachas, A. N. A., & Lewis, T. (2022). Drone-based  
779       environmental monitoring and image processing approaches for resource estimates of private  
780       native forest. *Sensors*, *22*(20), 7872.
- 781 Thakur, S., Maity, D., Mondal, I., Basumatary, G., Ghosh, P. B., Das, P., & De, T. K. (2021).  
782       Assessment of changes in land use, land cover, and land surface temperature in the mangrove  
783       forest of Sundarbans, northeast coast of India. *Environment, Development and Sustainability*,  
784       *23*(2), 1917–1943.
- 785 Tomlinson, P. B. (2016). *The botany of mangroves*. Cambridge University Press.
- 786 UNEP. (2023). *State of the world's mangroves 2023*. United Nations Environment Programme.  
787       <https://www.unep.org/resources/report/state-worlds-mangroves-2023>
- 788 Vadrevu, K. P., Eaturu, A., & Badarinath, K. (2010). Fire risk evaluation using multicriteria analy-  
789       sis—A case study. *Environmental Monitoring and Assessment*, *166*(1), 223–239.
- 790 Vaiphasa, C., Ongsomwang, S., Vaiphasa, T., & Skidmore, A. K. (2005). Tropical mangrove spe-  
791       cies discrimination using hyperspectral data: A laboratory study. *Estuarine, Coastal and Shelf*  
792       *Science*, *65*(1–2), 371–379.
- 793 Vyas, P., & Sengupta, K. (2012). Mangrove conservation and restoration in the Indian Sundarbans.  
794       In *Sharing lessons on mangrove restoration* (p. 93).
- 795 Ward, R. D., Friess, D. A., Day, R. H., & Mackenzie, R. A. (2016). Impacts of climate change  
796       on mangrove ecosystems: A region by region overview. *Ecosystem Health and Sustainability*,  
797       *2*(4), e01211.
- 798 Zhen, J., Mao, D., Shen, Z., Zhao, D., Xu, Y., Wang, J., Jia, M., Wang, Z., & Ren, C. (2024).  
799       Performance of xgboost ensemble learning algorithm for mangrove species classification with  
800       multisource spaceborne remote sensing data. *Journal of Remote Sensing*, *4*, 0146.

Alternative Texts for Your Images, Please Check and Correct them if Required

Page no	Fig/Photo	Thumbnail	Alt-text Description																						
	Fig1	 <p>A 3D pie chart titled "World's Mangrove Cover 2024" showing the distribution of mangrove coverage by region. The data is as follows:</p> <table border="1"> <thead> <tr> <th>Region</th> <th>Percentage</th> </tr> </thead> <tbody> <tr> <td>Southeast Asia</td> <td>33.6%</td> </tr> <tr> <td>West &amp; Central Africa</td> <td>15.5%</td> </tr> <tr> <td>North &amp; Central America &amp; Caribbean</td> <td>14.4%</td> </tr> <tr> <td>South America</td> <td>13.2%</td> </tr> <tr> <td>Australia &amp; New Zealand</td> <td>7.0%</td> </tr> <tr> <td>Pacific Islands</td> <td>3.9%</td> </tr> <tr> <td>East &amp; Southern Africa</td> <td>5.3%</td> </tr> <tr> <td>South Asia</td> <td>6.6%</td> </tr> <tr> <td>Middle East</td> <td>0.2%</td> </tr> <tr> <td>East Asia</td> <td>0.2%</td> </tr> </tbody> </table>	Region	Percentage	Southeast Asia	33.6%	West & Central Africa	15.5%	North & Central America & Caribbean	14.4%	South America	13.2%	Australia & New Zealand	7.0%	Pacific Islands	3.9%	East & Southern Africa	5.3%	South Asia	6.6%	Middle East	0.2%	East Asia	0.2%	<p>Pie chart titled “World’s Mangrove Cover 2024” showing the distribution of mangrove coverage by region. Southeast Asia has the largest share at 33.6%, followed by West &amp; Central Africa at 15.5%, North &amp; Central America &amp; Caribbean at 14.4%, and South America at 13.2%. Other regions include Australia &amp; New Zealand (7.0%), South Asia (6.6%), East &amp; Southern Africa (5.3%), Pacific Islands (3.9%), with East Asia and the Middle East both at 0.2%.</p>
Region	Percentage																								
Southeast Asia	33.6%																								
West & Central Africa	15.5%																								
North & Central America & Caribbean	14.4%																								
South America	13.2%																								
Australia & New Zealand	7.0%																								
Pacific Islands	3.9%																								
East & Southern Africa	5.3%																								
South Asia	6.6%																								
Middle East	0.2%																								
East Asia	0.2%																								
	Fig2	 <p>Two side-by-side maps of Sundarban, South 24-Parganas, West Bengal, India, showing land use and land cover in 1988 and 2022. The maps illustrate changes in categories such as forest, vegetation, river, waterbody, fallow land, agricultural land, and built-up area. A legend indicates the color coding for each category. The maps include scale bars and directional arrows for orientation.</p>	<p>Comparison of two geographical maps showing land use and land cover in Sundarban, South 24-Parganas, West Bengal, India for the years 1988 and 2022. The maps illustrate changes in categories such as forest, vegetation, river, waterbody, fallow land, agricultural land, and built-up area. A legend indicates the color coding for each category. The maps include scale bars and directional arrows for orientation.</p>																						